Two-Element T-Array for Cross-Polarized Breast Tumor Detection

H. Kanj and M. Popović

Department of Electrical and Computer Engineering
McGill University, 3480 University Street
Montreal, Quebec Canada H3A 2A7
houssam.kanj@mail.mcgill.ca, milica.popovich@mcgill.ca

Abstract – This paper reports on a computational study of a 2-element cross-polarized antenna array for breast cancer detection. The "Dark Eyes" antenna is used in a T-arrangement to form the array. The antenna return loss is below -10dB in the range 2.3-10.3 GHz and the cross-polarized mutual coupling is less than -30dB for frequencies over 2.4 GHz. Using the finite-difference time-domain (FDTD) method, an ultra-wideband (UWB) pulse is transmitted in the numerical breast phantom and the co- and cross-polarized back-scatter response is recorded from tumors at different locations. The breast phantom was modeled as a simple layered medium of skin and fat. The dispersive properties of layers were introduced through a Debye model. Simulation results for a spherical and a cylindrical tumor of different orientations are presented and discussed.

Keywords: Resistively loaded antennas, microwave imaging, cross-polarized array, breast cancer detection.

I. INTRODUCTION

Microwave imaging techniques are currently being studied as an effective low-cost screening tool for breast cancer detection systems [1, 2]. Furthermore, polarimetric radar-base imaging is thought to improve the imaging technique. For this application, several antennas have been suggested [3, 4]. However, most of these antennas are either large or nonplanar and thus difficult for use in an antenna array.

In a previous work, we have proposed an ultra-wideband (UWB) compact planar antenna design [5] that is easily fabricated using the standard printed circuit board (PCB) process with embedded resistive technology. The antenna can be manufactured on Rogers Duroid 6010 high frequency substrates [6] laminated with a resistive conductive material (RCM) available from Ohmega Technologies [7]. The key advantage of this antenna is its forward-region radiation pattern. This makes the antenna a perfect candidate for a cross-polarized card-array arrangement as suggested in [8]. In our work presented here, we extend our study [9] of the T-arrangement to be used as a sub-array unit for radar-based polarimetric breast cancer detection system.

The paper is organized as follows. Section II focuses on the geometry and characterization of T-arrangement for two "Dark Eyes" antennas in a homogeneous lossless medium. In Section III, we present a layered tissue model to assess near-field radiation characteristics of the antenna arrangement of Section II. Section IV offers a detailed study on the tumor detection levels as a function of the tumor shape and orientation (spherical, cylindrical − oriented in the cross- or co-polarized manner) and discusses the reported results. Finally, we make the concluding remarks and comment on our near-future work in Section V.

II. GEOMETRY AND CHARACTERIZATION OF THE TWO-ANTENNA T-ARRANGEMENT

Figure 1(a) shows the miniaturized "Dark Eyes" antenna reported in [5]. Figure 1(b) illustrates the proposed T-arrangement of two of these antennas in a cross-polarized configuration [8]. As the antenna is aimed to serve for microwave breast cancer detection, in our study, it is immersed in a lossless medium of relative permittivity $\epsilon_r = 10.2$ which is dielectrically close to that of the fatty breast tissue at the center of the frequency range under investigation [10]. The structure was simulated with SEMCAD [11] (three-dimensional finite-difference time-domain (FDTD) solver). The return loss S_{11} and mutual coupling S_{12} results were also verified with HFSS [12] (three-dimensional finite-element (FEM) solver).

We here report on the return loss and mutual coupling of the T-arrangement unit. The structure exhibits asymmetry and should be described by all three S-parameter values − S_{11}, S_{12}, and S_{22}, where the indices correlate with antenna numeration indicated in Fig. 1(b). Figure 2(a) shows that the Antenna-**1** return loss S_{11} in the 2.3-10.3GHz range and does not exceed -10dB. Nearly identical results (not shown here) are obtained for S_{22} (Antenna-**2** return loss). Another important parameter for array design is the mutual coupling. This is quantified by the S_{12} parameter graphed in Fig. 2(b). As can be observed, although the antennas were placed with only
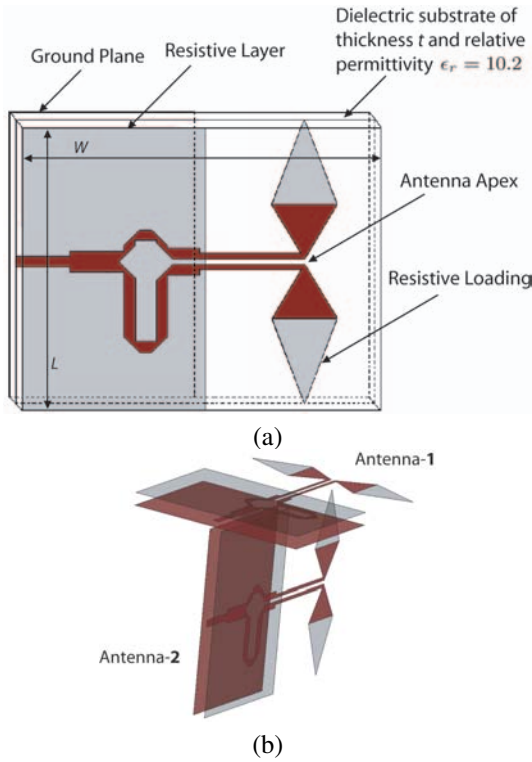
Fig. 1. (a) Geometry of the microstrip-fed resistively loaded "Dark Eyes" antenna. $L = 20 \ mm$, $W = 25 \ mm$, and $t = 0.65 \ mm$. Full description and analysis of the antenna can be found in [5]. (b) Proposed cross-polarized T-arrangement of the microwave sensing array unit, with "Dark Eyes" antenna from Fig. 1(a) as its main element [8].

Fig. 2. Simulated S-parameters for the T-arrangement of Fig. 1(b). (a) Input return loss characteristic S_{11}. (b) Mutual coupling S_{12}. Results are shown for SEMCAD (FDTD-based) and HFSS (FEM-based) simulation tools for comparison and verification.

11mm center-to-center spacing, the S_{12} is less than -30dB in the 2.4-11GHz range. These results suggest broadband behavior (low return loss and negligible mutual coupling) of the T-arrangement unit within the microwave range of interest for the intended application.

III. LAYERED TISSUE MODEL AND NEAR-FIELD RADIATION OF THE T-ARRANGEMENT

Figure 3 presents the simple layered tissue model of the breast. It consists of a matching medium, a 1-mm skin layer, and a fat medium. The T-arrangement is immersed in the matching medium which has a dielectric constant of $\epsilon_r = 10.2$. The skin, fat, and tumor tissue are modeled with a single-pole Debye dispersive medium defined as follows, [13]

$$\epsilon_r^*(w) = \epsilon_r'(w) - j\epsilon_r''(w) = \epsilon_\infty + \frac{\epsilon_s - \epsilon_\infty}{1 + jw\tau} - j\frac{\sigma_s}{w\epsilon_0} \quad (1)$$

where ϵ_∞ is the relative permittivity at infinite frequency, ϵ_s is the static relative permittivity, σ_s is the static conductivity, and τ is the relaxation time constant. Specific material properties for each tissue are presented in Table 1 [14]. These values are slightly higher than the
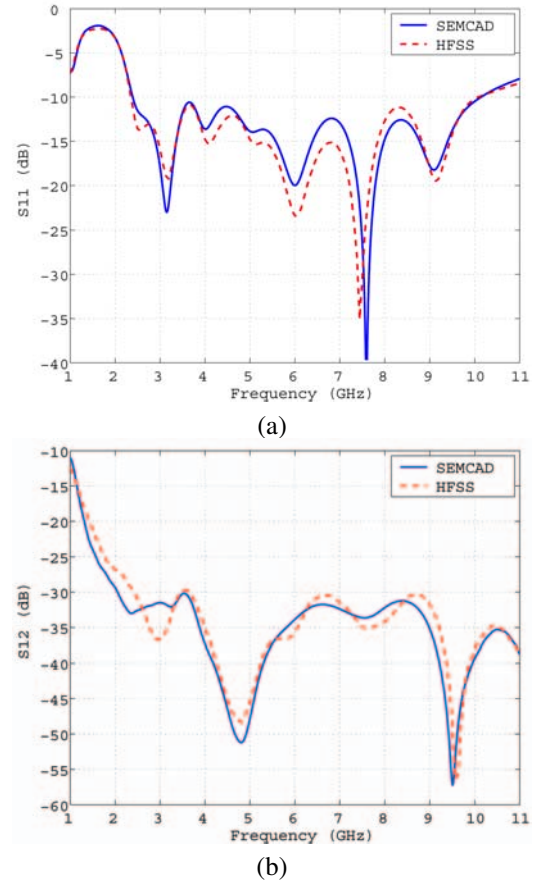
measured data for the high percentage adipose tissue recently reported in [15, 16].

Figure 3 shows 9 of the 25 simulated tumor locations alphabetically labeled 'a', 'b', ... 'i'. These locations, in addition to the other 16 not shown in the sketch, are evenly distributed on the portion of the sphere centered at Antenna-**1** apex. Therefore, the 25 points find themselves distributed along a "bowl-like" surface beneath Antenna-**1**. The choice of sampling field points over such a surface (as opposed to, e.g., a plane) was motivated by the fact that we are investigating near-field radiation,

Table 1. Material properties of the Debye dispersive model.

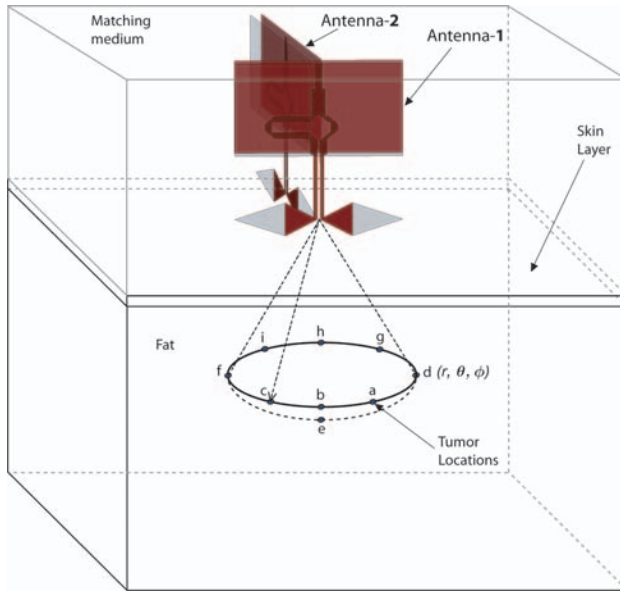| Tissue	Parameters			
	ϵ_∞	ϵ_s	σ_s(S/m)	τ(ps)
Skin	4.00	37.00	1.10	7.23
Tumor	3.99	54.00	0.70	7.0
Fat	7.00	10.00	0.15	7.0

Fig. 3. Layered model of the breast showing the T-arrangement, the matching medium, skin layer, fat, and 9 of the 25 simulated tumor locations.

where the wave has not yet acquired the plane-front of propagation. In all the simulations, the distance between the antenna apex and the skin is 5 mm. The tumor locations are also measured radially from the antenna apex with a radial distance of 3 cm.

Figure 4 shows near-field plots on the portion of the sphere inside the layered model. The plots are computed with HFSS and shown for three frequencies: (a) 3 GHz, (b) 6 GHz, and (c) 9 GHz. In these simulations, both antennas are present, however, only Antenna-**1** is active, while Antenna-**2** is passive. As we can see from the plots, the maximum intensity of the radiated electric field shifts toward the left side as the frequency increases. However, the range of the field magnitudes at all three frequencies is similar, approximately (2.5-5.5 V/m). This is important to the detection process as the antenna is supposed to radiate the energy uniformly in the intended direction.

IV. TUMOR RESPONSE STUDY OF THE T-ARRANGEMENT

In this section, the antenna array is used to study the co-polarized and cross-polarized response of different tumor shapes and orientations at various locations, summarized in Table 2. The antenna array was simulated using SEMCAD X [11]. The tumor was considered to be either a sphere of diameter $D = 5\ mm$ or a cylinder with a base diameter $D = 2.75\ mm$ and height $H = 5.5\ mm$. The chosen cylinder has its height equal to twice of its diameter ($H = 2D$), and it has the same volume as the chosen sphere. Finally, the cylinder is either oriented in parallel with Antenna-**1**, when we refer to it as Co-Cylinder, or it is oriented in parallel with Antenna-**2**, when it is called X-Cylinder. In this study, a tumor is
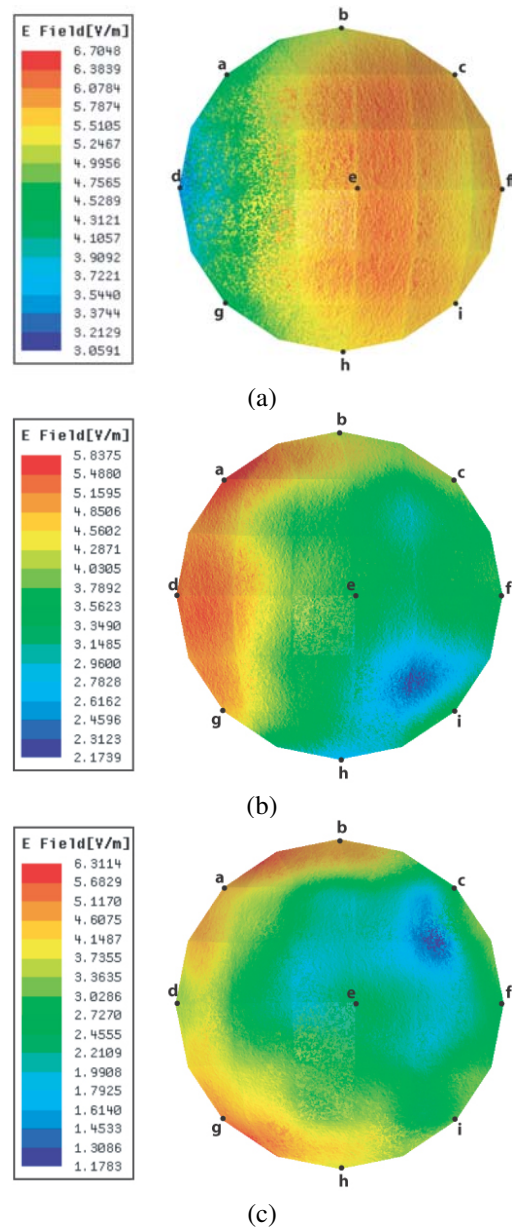

Fig. 4. Electric field magnitude at a radial distance of 30 mm from the antenna apex in the layered model of Fig. 3 at: (a) 3 GHz, (b) 6 GHz, (c) 9 GHz. In the simulations, the parameters of the fat layer containing the points for which the field is plotted are as follows: $\epsilon_r(3\text{GHz}) = 9.95$ and $\sigma(3\text{GHz}) = 0.21\text{S/m}$, $\epsilon_r(6\text{GHz}) = 9.8$ and $\sigma(6\text{GHz}) = 0.4\text{S/m}$, $\epsilon_r(9\text{GHz}) = 9.6$ and $\sigma(9\text{GHz}) = 0.66\text{S/m}$.

placed in the layered model at one of the 25 locations evenly distributed on the portion of a sphere shown in Fig. 3, and SEMCAD is used to compute the tumor response. Antenna-**1** is excited with a Gaussian modulated sinusoidal pulse described by,

$$\mathcal{V}(t) = \sin[2\pi f_0(t - t_0)] \exp\left[-\frac{(t - t_0)^2}{2\tau^2}\right], \quad (2)$$

with $f_0 = 6\text{GHz}$, $\tau = 80\text{ps}$, and $t_0 = 5\tau$, while Antenna-**2** is kept passive. To compute the tumor response

for each tumor location, two simulations are performed to obtain the voltage at the antenna feed: one with, and one without the tumor. By subtracting one simulated response from the other, skin reflection and early-time artifacts could be removed, providing the response of the tumor only. This is done for both antennas, Antenna-**1** and Antenna-**2**, to compute the co-polarized and cross-polarized tumor response, respectively.

Figure 5 shows the co-polarized and cross-polarized tumor response for the different tumor shapes and orientations considered within the spherical surface defined in Fig. 3. The presented results are the linear interpolation of the computed tumor response at the 25 simulated locations for each case. First, from Fig. 5 (a) and the computed data, we can see that the co-polarized tumor response for the sphere ranges from -88.6dB to -81.5dB (7.1dB). Our study confirms that the tumor response plot in this specific case correlates with the near-field radiation pattern of the "Dark Eyes" antenna. For the Co-Cylinder case shown in Fig. 5 (c), the co-polarized tumor response ranges from -90.2dB to -83.2dB (7.0dB), while for the X-Cylinder case shown in Fig. 5 (e), the co-polarized tumor response ranges from -94.8dB to -86.5dB (8.3dB).
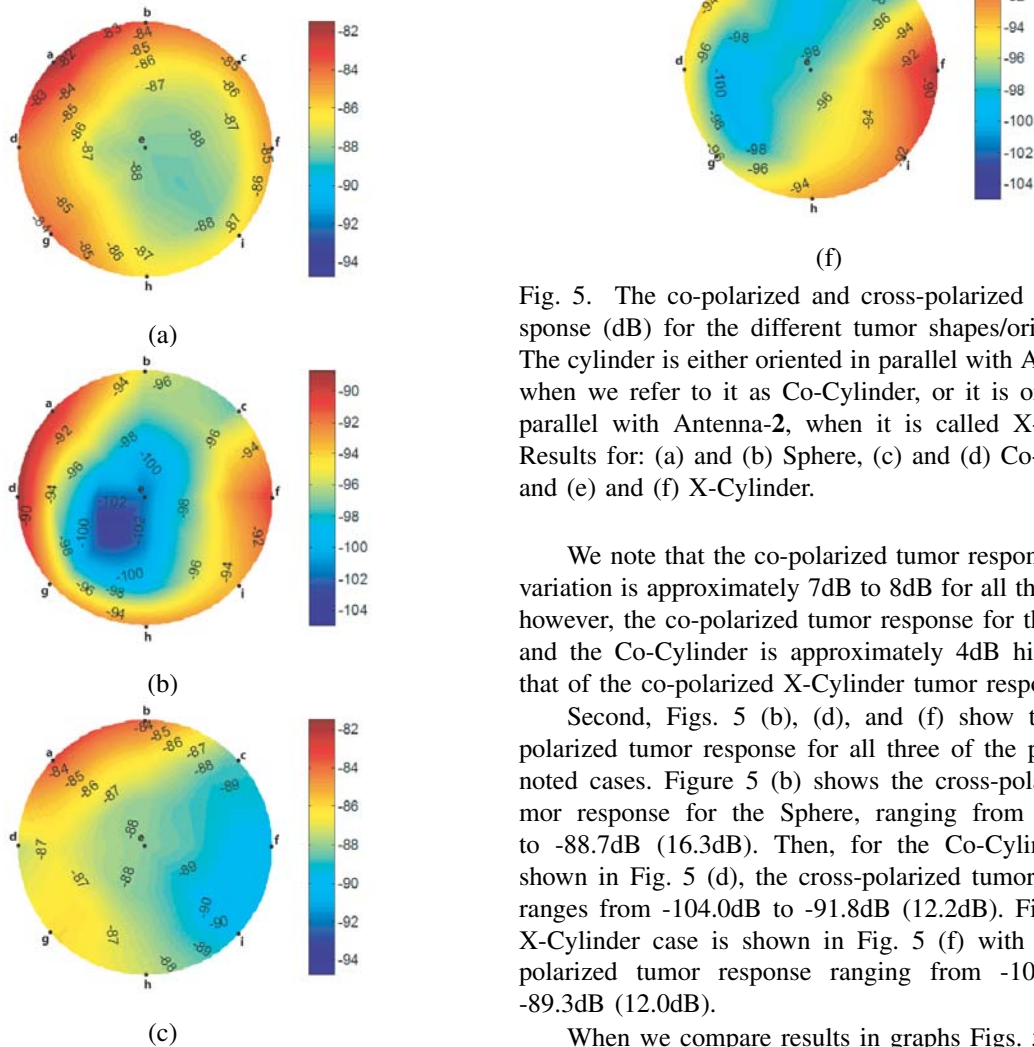

(a)

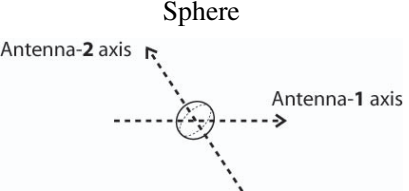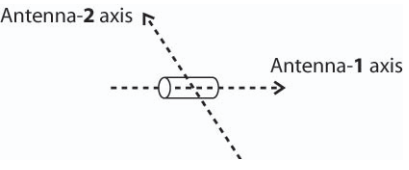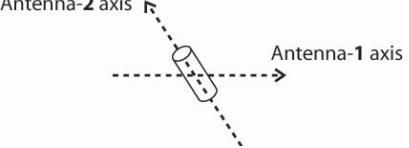
(b)

(c)

(d)

(e)

(f)

Fig. 5. The co-polarized and cross-polarized tumor response (dB) for the different tumor shapes/orientations. The cylinder is either oriented in parallel with Antenna-**1**, when we refer to it as Co-Cylinder, or it is oriented in parallel with Antenna-**2**, when it is called X-Cylinder. Results for: (a) and (b) Sphere, (c) and (d) Co-Cylinder, and (e) and (f) X-Cylinder.

We note that the co-polarized tumor response spatial variation is approximately 7dB to 8dB for all three cases, however, the co-polarized tumor response for the Sphere and the Co-Cylinder is approximately 4dB higher than that of the co-polarized X-Cylinder tumor response.

Second, Figs. 5 (b), (d), and (f) show the cross-polarized tumor response for all three of the previously noted cases. Figure 5 (b) shows the cross-polarized tumor response for the Sphere, ranging from -105.0dB to -88.7dB (16.3dB). Then, for the Co-Cylinder case shown in Fig. 5 (d), the cross-polarized tumor response ranges from -104.0dB to -91.8dB (12.2dB). Finally, the X-Cylinder case is shown in Fig. 5 (f) with its cross-polarized tumor response ranging from -101.3dB to -89.3dB (12.0dB).

When we compare results in graphs Figs. 5 (b), (d),

Table 2. Tumor response summary.

Tumor shape and orientation	Size (mm)	Co-pol response range (dB)	Cross-pol response range (dB)
Sphere — Antenna-2 axis, Antenna-1 axis	Diameter $D = 5$	$max = -81.5$ $min = -88.6$ $delta = 7.1$	$max = -88.7$ $min = -105.0$ $delta = 16.3$
Co-cylinder — Antenna-2 axis, Antenna-1 axis	Base Diameter $D = 2.75$ Height $H = 5.5$	$max = -83.2$ $min = -90.2$ $delta = 7.0$	$max = -91.8$ $min = -104.0$ $delta = 12.2$
Cross-cylinder — Antenna-2 axis, Antenna-1 axis	Base Diameter $D = 2.75$ Height $H = 5.5$	$max = -86.5$ $min = -94.8$ $delta = 8.3$	$max = -89.3$ $min = -101.3$ $delta = 12.0$

and (f) with Figs. 5 (a), (c), and (e), we can note that the co-polarized tumor response is always higher than that of the cross-polarized tumor response for the case of the Sphere and the Co-Cylinder. However, this is not the case for the X-Cylinder where the approximate 5.5dB overlap in the range of the co-polarized tumor response [-94.8dB to -86.5dB] and that of the cross-polarized tumor response [-101.3dB to -89.3dB] implies that having both co- and cross-polarization measurement may be advantageous for the overall detection process. This overlap in the co-polarized and cross-polarized tumor response is mainly attributed to the polarimetric signatures of the cylinder. Table 2 presents a summary of the tumor response study for all three cases under investigation.

V. CONCLUSIONS

This work presented an array arrangement of the "Dark Eyes" antenna for breast cancer detection. The antennas are arranged in a cross-polarized card array and exhibit low return loss (-10dB from 2.3GHz to 10.3GHz) and low mutual coupling (-30dB from 2.4GHz to 11GHz) even when placed in the very proximity of each other. The near-field radiation patterns at 3GHz, 6GHz, and 9GHz were also presented and the results show that the radiated energy is better directed to the forward region of the antenna at the lower frequency range. Further, a computational study of the tumor response for different tumor shapes and orientations was executed in a simple layered breast model. Both, the co-polarized and the cross-polarized backscatter was recorded from the tumor placed at different locations in the forward region of the antenna array. The initial results indicate that when looking at the co-polarized response, it is the Sphere and the Co-Cylinder that provided higher-amplitude response. On the other hand, when looking at the cross-polarized response, it is the X-Cylinder that provided the higher-amplitude response. Thus, for extracting maximum information about the tumor, and since the tumor shape and orientation are unknown, there is an advantage in using the cross-polarized array arrangement.

REFERENCES

[1] Y. Xie, B. Guo, L. Xu, J. Li, and P. Stoica, "Multistatic adaptive microwave imaging for early breast cancer detection," *IEEE Transactions on Biomedical Engineering*, vol. 53, pp. 1647–1657, August 2006.

[2] D. J. Kurrant, E. C. Fear, and D. T. Westwick, "Tumor estimation in tissue sensing adaptive radar (tsar) signals," in *Canadian Conference on Electrical and Computer Engineering*, 2007.

[3] S. C. Hagness, A. Taflove, and J. E. Bridges, "Three-dimensional FDTD analysis of a pulsed microwave confocal system for breast cancer detection: Design of an antenna-array element," *IEEE Trans. Antennas Propagat.*, vol. 47, pp. 783–791, May 1999.

[4] X. Yun, E. C. Fear, and R. H. Johnston, "Compact antenna for radar-based breast cancer detection," *IEEE Trans. Antennas Propagat.*, vol. 53, pp. 2374–2380, August 2005.

[5] H. Kanj and M. Popovic, "Miniaturized microstrip-fed "Dark Eyes" antenna for near-field microwave sensing," *IEEE Antennas Wireless Propagat. Lett.*, vol. 4, pp. 397–401, 2005.

[6] (2007) Rogers website. [Online]. Available: http://www.rogerscorporation.com

[7] (2007) Ohmega website. [Online]. Available: http://www.ohmega.com/

[8] H. Kanj and M. Popovic, "T- and X-arrangement of "Dark Eyes" antennas for microwave sensing array," in *Proc. IEEE AP-S International Symposium*, Albuquerque, NM, pp. 1111–1114, July 2006.

[9] ——, "Two-element T-array for cross-polarized breast tumor detection," in *The 23rd Annual Review of Progress in Applied Computational Electromagnetics*, Verona, Italy, pp. 846–850, March 2007.

[10] S. Gabriel, R. W. Lau, and C. Gabriel, "The dielectric properties of biological tissues-ii: Measurements on the frequency range 10 Hz to 20 GHz," *Physics in Medicine and Biology*, vol. 41, pp. 2251–2269, November 1996.

[11] (2007) SEMCAD website. [Online]. Available: http://www.semcad.com/

[12] (2007) Ansoft website. [Online]. Available: http://www.ansoft.com/

[13] A. Taflove and S. Hagness, Eds., *Computational Electrdynamics: The Finite-Difference Time-Domain Method*. Boston, MA: Artech House, 2005.

[14] M. Converse, E. J. Bond, B. D. Van Veen, and S. C. Hagness, "A computational study of ultra-wideband versus narrowband microwave hyperthermia for breast cancer treatment," *IEEE Trans. Microwave Theory Tech.*, vol. 54, pp. 2169–2180, May 2006.

[15] M. Lazebnik, L. McCartney, D. Popovic, C. B. Watkins, M. J. Lindstrom, J. Harter, S. Sewall, A. Magliocco, J. H. Booske, M. Okoniewski, and S. C. Hagness, "A large-scale study of the ultrawideband microwave dielectric properties of normal breast tissue obtained from reduction surgeries," *Physics in Medicine and Biology*, vol. 52, pp. 2637–2656, 2007.

[16] M. Lazebnik, D. Popovic, L. McCartney, C. B. Watkins, M. J. Lindstrom, J. Harter, S. Sewall, T. Ogilvie, A. Magliocco, T. M. Breslin, W. Temple, D. Mew, J. H. Booske, M. Okoniewski, and S. C. Hagness, "A large-scale study of the ultrawideband microwave dielectric properties of normal, benign and malignant breast tissues obtained from cancer surgeries," *Physics in Medicine and Biology*, vol. 52, pp. 6093–6115, 2007.

Houssam Kanj received his B.Sc. in Computer and Communication Engineering from The American University of Beirut in 1999, the M.Sc. in Electrical Engineering from North Carolina State University in 2003, and the Ph.D. degree in Electrical Engineering from McGill University in 2008. His Masters research was in the fields of analog circuit design and computer-aided modeling of nonlinear circuits including electro-thermal and lasers. His current research interests include numerical methods in electromagnetics for bio-medical applications and antenna design.

Milica Popović received her B.Sc. (1994) from University of Colorado (Boulder, Colorado, USA) and M.Sc. (1997) and Ph.D. (2001) degrees from Northwestern University (Evanston, Illinois, USA), all in electrical engineering. She is currently an associate professor with the Department of Electrical and Computer Engineering at McGill University in Montral, Canada. Her research interests focus on numerical methods in computational electromagnetics for bio-medical applications, in particular: breast cancer screening with microwaves, wireless implants for physiological research and light interaction with retinal photoreceptor cells. On the teaching side, her efforts include improvement methods for instruction of introductory electromagnetics courses.